Amyloid Fibril Formation Requires a Chemically Discriminating Nucleation Event: Studies of an Amyloidogenic Sequence from the Bacterial Protein OsmB†

Joseph T. Jarrett and Peter T. Lansbury, Jr.*

Department of Chemistry, Massachusetts Institute of Technology, Cambridge, Massachusetts 02139

Received July 31, 1992; Revised Manuscript Received September 25, 1992

ABSTRACT: The sequence of the *Escherichia coli* OsmB protein was found to resemble that of the C-terminal region of the β amyloid protein of Alzheimers's disease, which seems to be the major determinant of its unusual structural and solubility properties. A peptide corresponding to residues 28–44 of the OsmB protein was synthesized, and its conformational properties and aggregation behavior were analyzed. The peptide OsmB(28–44) was shown to form amyloid fibrils, as did two sequence analogs designed to test the sequence specificity of fibril formation. These fibrils bound Congo red, and two of the peptides showed birefringence. The peptide fibrils were analyzed by electron microscopy and Fourier transform infrared spectroscopy. Subtle differences were observed which were not interpretable at the molecular level. The rate of fibril formation by each peptide was followed by monitoring the turbidity of supersaturated aqueous solutions. The kinetics of aggregation were characterized by a delay period during which the solution remained clear, followed by a nucleation event which led to a growth phase, during which the solution became viscous and turbid due to the presence of insoluble fibrils. The observation of a kinetic barrier to aggregation is typical of a crystallization event. The delay period could be eliminated by seeding the supersaturated solution with previously formed fibrils. Each peptide could be nucleated by fibrils formed from that same peptide, but not by fibrils from closely related sequences, suggesting that fibril growth requires specific hydrophobic interactions. It appears likely that this repeated sequence motif, which comprises most of the OsmB protein sequence, dictates the structure and possibly the function of that protein. While amyloid formation was shown not to require this sequence, similarities in sequence and composition between OsmB and the β amyloid protein may be significant. Furthermore, these studies demonstrate that amyloid fibril formation is chemically discriminating, and that nucleation of fibril formation is the rate-limiting step in amyloidogenesis. This finding has important ramifications for the understanding of amyloid formation in Alzheimer's disease.

The presence of extracellular amyloid plaque is characteristic of the Alzheimer's disease brain. The plaque is composed primarily of a single protein known as the β amyloid protein (Glenner & Wong, 1984; Masters et al., 1985), which is derived from the putative transmembrane region of its precursor protein, βAPP[1] (Dyrks et al., 1988; Kang et al., 1987). We have shown that a peptide comprising the C-terminal nine amino acids of the β protein (β(34–42)) forms amyloid fibrils (Halverson et al., 1990), suggesting that this region of the β protein may be critical for the formation of fibrils in vivo. Subsequent studies have confirmed the importance of the C-terminal sequence (Burdick et al., 1992; Hilbich et al., 1991). The premise of the studies described herein is that the C-terminus of the β protein contains a primary and/or secondary structural motif which may occur in other amyloidogenic proteins.

The C-terminal region of the β protein contains 14 consecutive hydrophobic residues, consistent with its location within the putative transmembrane region of the βAPP. The prevalence of the β-branched residues valine and isoleucine is striking. In addition, the regular occurrence of glycine at every fourth residue is reminiscent of the silk protein sequences, which contain the consensus sequence $(GAGS)_n$ (Fraser & MacRae, 1973). The conformational flexibility of the Gly residue may allow the polypeptide chain to adopt conformations which are not normally populated in crystalline proteins (Chou et al., 1982; Richardson & Richardson, 1989). Consecutive Gly residues may allow unusual local conformations such as cis amide bonds (Spencer et al., 1991). In order to search the sequence database for proteins containing sequences similar to that of the β protein, we developed a hypothetical consensus sequence for amyloid formation on the basis of the three characteristics summarized above: the overall hydrophobicity, the occurrence of glycine at every fourth residue, and the frequent occurrence of β-branched residues.

A search of the protein sequence database uncovered 27 proteins which contained sequences fulfilling the general criteria outlined above and detailed below. These include a region of the scrapie prion protein (residues 96–111), which is known to form amyloid fibrils (Stahl & Prusiner, 1991). The *Escherichia coli* OsmB protein contains two similar sequence repeats, comprising ca. 70% of the 49-residue protein (Jung et al., 1989). OsmB is a periplasmic outer membrane-associated lipoprotein, which is upregulated in response to osmotic stress. Its function is unknown, but it has been

† This work was supported by grants from the Procter and Gamble Co. (University Exploratory Research Program) and The National Institutes of Health (AG08470). P.T.L. is the Firmenich Assistant Professor of Chemistry, a Sloan Research Fellow, and a Camille and Henry Dreyfus Teacher–Scholar. J.T.J. is an NIH predoctoral trainee (1T32GM-08318-01).

[1] Abbreviations: βAPP, β amyloid precursor protein; AD, Alzheimer's Disease; BCA, bicinchoninic acid; BOP, (benzotriazol-1-yloxy)tris-(dimethylamino)phosphonium hexafluorophosphate; CD, circular dichroism spectroscopy; DIEA, diisopropylethylamine; DMF, dimethylformamide; DMSO, dimethyl sulfoxide; EM, electron microscopy; FAB MS, fast atom bombardment mass spectrometry; FTIR, Fourier transform infrared spectroscopy; HFIP, 1,1,1,3,3,3-hexafluoro-2-propanol; HPLC, high-performance liquid chromatography; TFA, trifluoroacetic acid; TFE, 2,2,2-trifluoroethanol.

0006-2960/92/0431-12345$03.00/0

suggested that it plays a role in reinforcing the outer membrane, preventing cell death during sudden osmotic changes (Jung et al., 1989).

We have synthesized a peptide corresponding to residues 28–44 of the OsmB protein in order to investigate the hypothesis that this sequence motif drives amyloid formation. The conformational behavior of this peptide and two related peptides was studied in solution (CD) and in the solid state (EM, FTIR). The aggregation and dissolution kinetics were measured, and the specificity of the aggregation was examined. The results reported herein are relevant to understanding the in vivo formation and growth of amyloid plaque.

MATERIALS AND METHODS

Materials. The Rink amide methylbenzhydrylamine resin (substitution 0.6 mmol/g) was obtained from Novabiochem. BOP[1] reagent was obtained from Richelieu Biotechnologies. DIEA was obtained from Aldrich Chemical and distilled from ninhydrin under reduced pressure. BCA protein assay was obtained from Pierce Chemical. Millex-GV 0.22-μm filters were obtained from Millipore.

Protein Sequence Search. The CAS Online protein sequence database was searched for proteins which contained a repeating GXXX motif. At least 3 glycines (12 residues) were required. The nonglycine residues were allowed to be virtually any uncharged residue (G, A, V, I, L, F, W, Y, T, S, or M). Proline was not allowed since it disrupts β-sheet structure (Chou & Fasman, 1978). Eighty sequences were found. Sequences containing polyglycine and long GXGX repeats (silk proteins) were eliminated. The remaining sequences were screened for those that were relatively hydrophobic (hydropathy $\geq$ 1.4; Kyte & Doolittle, 1982) and contained residues often found in β-sheets but rarely in α-helices in globular proteins ($P_\beta - P_\alpha \geq 0.17$; Chou & Fasman, 1978). Twenty-seven sequences survived including the β amyloid protein (residues 29–40), the scrapie prion protein (residues 96–111), and the *E. coli* OsmB protein (residues 14–25 and 28–44) (Figure 1).

Peptide Synthesis, Purification, and Characterization. Peptides were synthesized manually on the Rink amide resin using commercially available Fmoc-amino acids. The side chains of serine and threonine were protected as the *t*-butyl ethers. Fmoc-peptide–resin was deprotected with 50% piperidine/DMF for 15 min. Coupling was achieved with 3 equiv of amino acid, 3 equiv of BOP, and 6 equiv of DIEA in DMF for 1 h. Couplings were monitored by the Kaiser test (Kaiser et al., 1970). After coupling and deprotection of the final residue, the N-terminus was acetylated with acetic anhydride and DIEA (10 equiv each in dichloromethane, 4 h). The resin-bound peptides were cleaved and deprotected with neat trifluoroacetic acid (30 min, 23 °C). The resin was filtered and washed with TFA and CH_2Cl_2. The combined filtrates were concentrated, and the peptide was precipitated by addition dropwise to cold diethyl ether (100 mL). The precipitates were collected by centrifugation, washed with additional ether, and dried. The crude solid was dissolved inHFIP and purified by reverse-phase HPLC under isocratic conditions on a C_4 semipreparative column (YMC, 2.0 × 25 cm) using H_2O + 0.1% TFA and acetonitrile + 0.1% TFA as eluents. The collected fractions were concentrated in vacuo and lyophilized to yield the peptide as a white solid. The purity of each peptide was confirmed by reverse-phase HPLC under isocratic conditions on a C_4 analytical column (Waters, 0.39 × 30 cm). Quantitative amino acid analysis was performed on HFIP solutions of the pure peptide using arginine as an internal standard.[2] The solution was dried, and the peptide hydrolyzed with 6 N HCl + 0.1% phenol (110 °C for 24–48 h). The samples were then derivatized with phenyl isothiocyanate and analyzed using the Waters Picotag system. Peptides were analyzed by both Plasma Desorption and FAB mass spectrometry.[2] A single parent ion corresponding to $M + H^+$ or $M + Na^+$ was observed for each peptide, and the fragmentation pattern observed in the FAB mass spectrum verified the sequence. ^{1}H NMR spectra in DMSO solution were recorded for each peptide and were consistent with the proposed structure.[2]

Peptide Solubility. Attempts to determine the solubility of each peptide by directly dissolving the lyophilized peptide gave erratic results. To determine the thermodynamic solubility of each peptide, a supersaturated solution of the peptide in 100 mM NaCl, 8.2 mM Na_2HPO_4, 1.8 mM NaH_2PO_4 (pH 7.4, hereafter referred to as the standard buffer) was stirred to initiate aggregation and then allowed to aggregate and equilibrate over 3–4 weeks (as described in the kinetics section below). The aggregate was removed by centrifugation, and the supernatant was filtered through Millex-GV 0.22-μm aqueous filters. Peptide concentration was determined by the BCA protein assay (Smith et al., 1985) using standards of the same peptide which had been previously calibrated by quantitative amino acid analysis. Results were reproducible to within ±5%.

Congo Red Staining and Birefringence. A suspension of peptide fibrils in water was allowed to dry on a glass microscope slide. The peptide film was immersed in a solution containing 1 mM Congo red, 100 mM NaCl, 10 mM phosphate, pH 7.4, for 1 min and then rinsed by immersing in distilled water for 1 min and dried. Birefringence was determined with a Wild Leitz M3Z light microscope equipped with a polarizing stage.

Circular Dichroism Spectroscopy. Circular dichroism spectra were recorded on an AVIV 60DS spectrapolarimeter in the laboratory of Dr. Robert Sauer, Department of Biology, MIT. Quartz cells of 0.1-cm path length were obtained from Hellma; 0.01- and 0.001-cm path length cells were obtained from Starna. A stock solution of each peptide ($\sim$1 mM) was prepared in HFIP. The exact concentrations were determined by quantitative amino acid analysis. Aliquots of this solution were transferred to 1.5-mL Eppendorf tubes, and the HFIP was removed in vacuo. The peptide was dissolved in the appropriate solvent by sonicating for several seconds. The standard buffer used for CD was 100 mM KF, 8.2 mM K_2HPO_4, 1.8 mM KH_2PO_4, pH 7.4. In some cases, the solution was supersaturated but did not aggregate during the CD experiment. Each sample was scanned three times from 250 to 190 nm, with 1-nm steps and 1.0-s averaging. Solvent and

[2] OsmB(28–44): amino acid analysis S 0.9(1), G 7.0(7), T 1.8(2), A 2.0(2), V 1.6(2), I 0.8(1), L 2.3(2); FABMS 1428.0 (calcd 1427.8); NMR (characteristic resonances only) 0.80 (m, 30 H, Leu, Ile, Val CH_3), 1.04 (m, 6 H, Thr CH_3), 1.20 (d, 6 H, J = 7.0 Hz, Ala CH_3), 1.5–1.7 (m, 9 H, Leu, Ile βH and γH), 1.85 (s, 3 H, acetyl), 1.95 (m, 2 H, J = 6.5 Hz, Val βH), 7.05 (s, 1 H, $CONH_2$), 7.17 (s, 1 H, $CONH_2$), 7.6–8.2 (m, 17 H, NH). OsmG3: amino acid analysis S 0.9(1), G 7.6(7), T 2.0(2), A 2.0(2), V 1.9(2), I 0.9(1), L 2.3(2); FABMS 1427.8 (calcd 1427.8); NMR 0.80 (m, 30 H, Leu, Ile, Val CH_3), 1.05 (m, 6 H, Thr CH_3), 1.20 (t, 6 H, J = 7.0 Hz, Ala CH_3), 1.5–1.7 (m, 9 H, Leu, Ile βH and γH), 1.83 (s, 3 H, acetyl), 1.95 (m, 2 H, J = 6.5 Hz, Val βH), 7.07 (s, 1 H, $CONH_2$), 7.21 (s, 1 H, $CONH_2$), 7.7–8.2 (m, 17 H, NH). OsmA: amino acid analysis S 1.1(1), G 4.4(4), T 1.9(2), A 4.9(5), V 1.8(2), I 0.9(1), L 2.4(2); FABMS 1469.8 (calcd 1469.8); NMR 0.80 (m, 30 H, Leu, Ile, Val CH_3), 1.04 (m, 6 H, Thr CH_3), 1.2 (m, 15 H, Ala CH_3), 1.6–1.8 (m, Leu, Ile βH and γH), 1.83 (s, 3 H, acetyl), 1.95 (m, 2 H, J = 7.1 Hz, Val βH), 7.05 (s, 1 H, $CONH_2$), 7.17 (s, 1 H, $CONH_2$), 7.6–8.2 (m, 17 H, NH).

cell backgrounds were subtracted from each sample. Spectra were recorded at 25 °C except where noted. Secondary structural analysis was performed by the method of Morrisett (Morrisett et al., 1973; Greenfield & Fasman, 1969), which is based on reference spectra derived from polylysine.

Fourier Transform Infrared Spectroscopy. Aggregated peptides were collected by centrifugation and spread evenly on a CaF_2 plate. After air drying, excess salt was removed by soaking the solid in H_2O for 1 min. The remaining aggregate was dried in vacuo. The spectra were recorded on a Perkin-Elmer FTIR spectrometer. The interferograms from 16 scans were averaged, and the contribution from air was subtracted. Spectra were routinely smoothed to improve the signal to noise ratio. Peak positions were determined with the aid of second-derivative analysis.

Electron Microscopy. Peptides were aggregated as described below in the standard phosphate buffer at 200–400 μM. Small aliquots of suspended aggregate were placed on carbon-coated copper grids and stained with 2% (w/v) uranyl acetate. Samples were viewed in a JOEL 1200CX electron microscope operating at 80 kV, typically at 60K–120K magnification.

Kinetic Aggregation Studies. In order to prepare a supersaturated aqueous solution from which aggregation could occur, each peptide was first dissolved in HFIP at 1–2 mM and then the HFIP was removed, either with a gentle stream of nitrogen or in vacuo, until the peptide formed a clear film. This film could be redissolved in Milli-Q water, resulting in 0.2-1 mM solutions. Further drying of the HFIP film resulted in a less soluble white solid. The peptide solution was then filtered through 0.22-μm filters, and the concentration was determined by the BCA assay. The solutions were used immediately in aggregation assays, since delays of more than a few hours resulted in partial aggregation of these stock solutions. The peptide solutions were diluted to the appropriate concentration in 900 μL of H_2O, and a concentrated salt solution (1 M NaCl, 82 mM Na_2HPO_4, 18 mM NaH_2PO_4, pH 7.4, 100 μL) was added, to afford the standard buffer conditions. The addition of salt was considered the initiation point for aggregation. Turbidity data were collected at 400 nm vs a blank containing the buffer solution only. The peptide solutions were vortexed slightly before each absorbance measurement to distribute the peptide fibrils evenly throughout the solution. Prolonged agitation was avoided as it was found to accelerate peptide aggregation. To determine the ability of each peptide aggregate to redissolve, 250 μM solutions of each peptide in buffer (1 mL) were aggregated by stirring for 15 h. The aggregates were pelleted by centrifugation, the supernatant was removed, and fresh buffer (1 mL) was added. The tube was vortexed to evenly suspend the fibrils and allowed to equilibrate for 5 days. At this time, the remaining aggregate was removed by centrifugation, the supernatant was filtered through 0.22-μm filters, and the peptide concentration was determined by the BCA assay. To study the kinetics of nucleated growth, the peptide aggregates were formed by stirring 250 μM solutions for 15 h. These aggregates were sonicated for several minutes, and an aliquot of this fibril suspension (50 μL, 12.5 nmol) was added to 950 μL of a 250 μM peptide in buffer solution. The solution was vortexed and the turbidity was monitored at 400 nm for 30 min with no further agitation.

RESULTS

A Sequence Search Reveals Proteins Which Share Similar Hydrophobic Sequences. A consensus sequence was developed on the basis of the C-terminal region of the β amyloid protein. The CAS Online protein sequence database was searched for proteins which contained at least three repeats (12 residues) of the GXXX sequence (X is G, A, V, I, L, F, W, Y, T, S, or M). This sequence would occur randomly in about 1 in 1 000 000 12-residue sequences. The 80 sequences initially discovered were screened for those that were hydrophobic and contained residues found predominantly in β-sheets. The C-terminus of the β amyloid protein remained, along with 26 other sequences, including one from the scrapie prion protein (residues 96–111) (Stahl & Prusiner, 1991) and a repeated sequence from the *E. coli* OsmB protein (residues 14–25 and 28–44) (Jung et al., 1989) (Figure 1).

β protein (29-42):	...GAIIGLMVGGVVIA-CO_2H
Prion Protein (96-111):	...AGAVVGGLGGYMLGSA...
OsmB Protein (14-25):	...GAGAGALGGAVL...
OsmB Protein (28-44):	...GSTLGTLGGAAVGGVIG...

FIGURE 1: Sequence of β amyloid protein showing the GXXX sequence repeat, along with the scrapie prion protein and two regions from the OsmB protein.

OsmB(28-44):	AcNH-GSTLGTLGGAAVGGVIG-$CONH_2$
OsmG3:	AcNH-GSTGLTGLAGAVGVIGG-$CONH_2$
OsmA:	AcNH-GSTLATLGAAAVAGVIG-$CONH_2$

FIGURE 2: Sequences of the peptides studied.

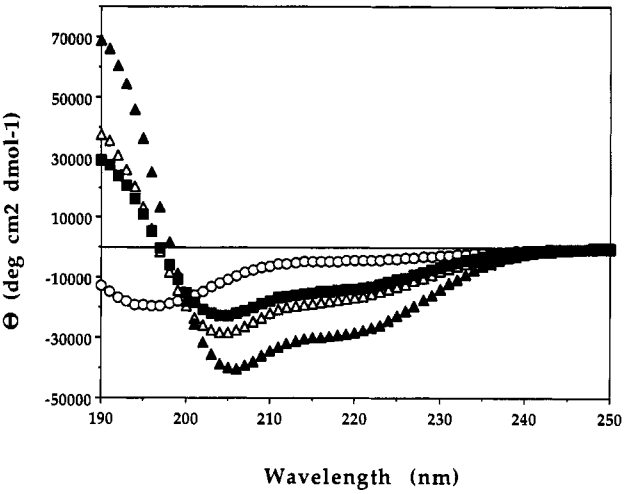

FIGURE 3: Circular dichroism of peptides at 100 μM: (○) OsmB-(28–44) in aqueous buffer; (△) OsmB(28–44) in 30% HFIP; (■) OsmG3 in 30% HFIP; (▲) OsmA in 30% HFIP.

Control Peptides Were Designed To Test the Importance of Sequence. In order to test the hypothesis that the occurrence of Gly at every fourth residue is critical for amyloidogenesis, two control peptides with slightly altered sequences were synthesized (Figure 2). The control peptide OsmG3 has an amino acid composition which is identical to OsmB(28–44); however, the sequence was permuted to create a peptide with glycine at every third residue. The control peptide OsmA contains three Gly to Ala "mutations" (Figure 2).

The Peptides Exist as a Mixture of Conformers in Dilute Aqueous Solution but Take on a Helical Conformation in Nonpolar and Amphipathic Media. The CD spectrum of each peptide (100 μM) in buffer (Figure 3) was consistent with a "random-coil" conformation (Greenfield & Fasman, 1969). OsmB is upregulated in *E. coli* during osmotic stress (0.4 M NaCl in the extracellular medium) (Jung et al., 1989); however, no conformational changes were observed for any of the peptides at high salt (1 M KF). Addition of TFE or HFIP to aqueous peptide solutions induced α-helical con-

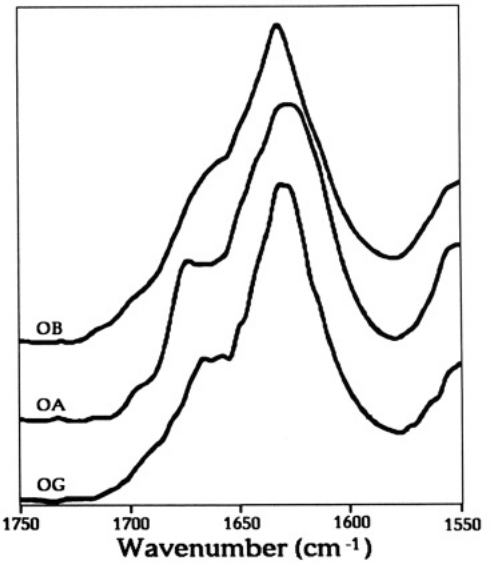

FIGURE 4: FTIR of fibrils formed by stirring a supersaturated aqueous solution: (OB) OsmB; (OG) OsmG3; (OA) OsmA.

formations (Figure 3). The characteristic CD spectra show a minimum at 204 nm and an inflection at 220 nm (Morrisett et al., 1973). Maximum structure was observed in 90% (v/v) TFE and in 30% (v/v) HFIP. In 30% HFIP, OsmB(28–44) was 48% helical, OsmG3 was 41% helical, and OsmA was 77% helical (Figure 3). The increased helicity in OsmA is consistent with the relative helix propensities of Gly and Ala (Ananthanarayanan et al., 1971; Marquesee et al., 1989). Sodium dodecyl sulfate (5% w/v) solutions of each peptide demonstrated levels of helicity comparable to those observed in 30% HFIP.

The Peptides Undergo a Concentration-Dependent Transition to β-Structure. The CD spectrum of each of the peptides was recorded at increasing peptide concentration (10–2000 μM) in H_2O. The concentration of OsmB(28–44) can be increased to ~1 mM (ca. 20-fold supersaturated) with no significant change in the CD spectrum. The shape of this spectrum is identical to that observed for OsmB(28–44) in aqueous buffer (Figure 3). At higher concentrations, the peptide forms a gel, with a concomitant decrease in the CD signal but with no change in the shape of the spectrum. FTIR of the gel shows a strong band at ca. 1630 cm^{-1}, suggesting the presence of antiparallel β-sheet structure (Krimm & Bandekar, 1986). The control peptides have similar behavior, with the spontaneous gel transition occurring at ~1.2 mM for OsmG3 and at ~0.5 mM for OsmA.

Peptides Aggregate from Supersaturated Solution To Form Fibrils Containing β-Structure. Metastable supersaturated solutions of each peptide could be prepared in water as described above. These solutions were stable for hours to days depending upon the degree of supersaturation. Agitation of these solutions by stirring or sonication caused aggregation to occur with little or no delay. The degree of aggregation could be followed by measuring the turbidity of the solutions, and generally approached an equilibrium within 1–2 h. The aggregates were collected by centrifugation, spread on an CaF_2 IR plate, and dried. The FTIR spectra (Figure 4) showed major bands at ca. 1630 and 1695 cm^{-1}, indicative of antiparallel β-sheet structure, as well as a band at 1665 cm^{-1}, which may be due to β-turn structure (Krimm & Bandekar, 1986). The solubility of each peptide in H_2O after aggregation was OsmB(28–44), 50 μM; OsmG3, 83 μM; and OsmA, 13 μM.

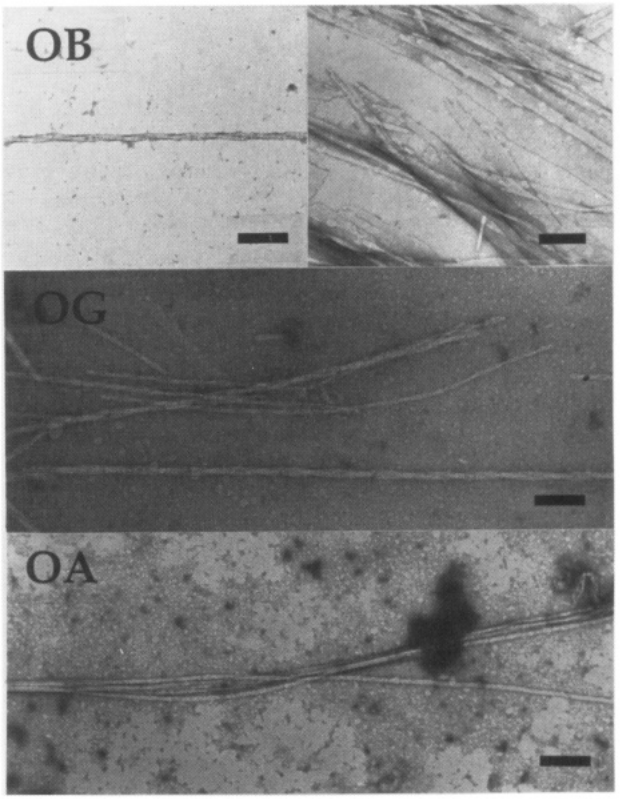

FIGURE 5: Electron micrographs of peptide fibrils: (OB) OsmB; (OG) OsmG3; (OA) OsmA. Bar = 1000 Å.

The aggregates from each peptide were studied by electron microscopy (Figure 5). The morphology of the peptide fibrils varied considerably. OsmB(28–44) formed twisted fibrils 100–150 Å in diameter, with a twist periodicity of 1300 ± 100 Å. These fibrils aggregated in two distinct forms, depending on peptide concentration. In more dilute samples (<500 μM), two fibrils twisted around each other in a helical manner with a periodicity of 1800 Å. In concentrated samples, the fibrils tended to clump into ribbon-like structures containing 20–30 fibrils, with each ribbon about 200 × 1000 Å in cross-section and several thousand nanometers long; these ribbons also clumped strongly together. OsmG3 formed fibrils which were similar to those from OsmB(28–44) with respect to width and twist periodicity; however, the OsmG3 fibrils tended to wind together in larger fibrils containing 2–5 smaller fibrils. OsmA formed straight rods, also about 100 Å in diameter, with no observable twist. These clumped together in a parallel manner, but with no distinguishable higher-level order. The aggregates of each peptide were also tested for Congo red binding and birefringence. All of the peptide aggregates bound Congo red, resulting in reddish-pink films. After staining, both OsmB(28–44) and OsmA exhibited yellow-green birefringence; however, stained OsmG3 was not birefringent.

The Aggregation Kinetics Are Characterized by Slow Nucleation Followed by Rapid Growth. Peptide solutions in water could be further supersaturated by the addition of a small aliquot of a concentrated salt solution. The final salt conditions (100 mM NaCl, 10 mM phosphate) and pH (7.4) were close to physiological. The final peptide concentrations were 250–500 μM, which is ~10-fold higher than the equilibrium solubilities measured under these conditions. The resulting peptide solutions were allowed to equilibrate undisturbed. OsmA initially appeared to be soluble, but aggregated after several hours, resulting in an increase in the turbidity of the solution (Figure 6). OsmB(28–44) and OsmG3 showed no aggregation for several days by either visual

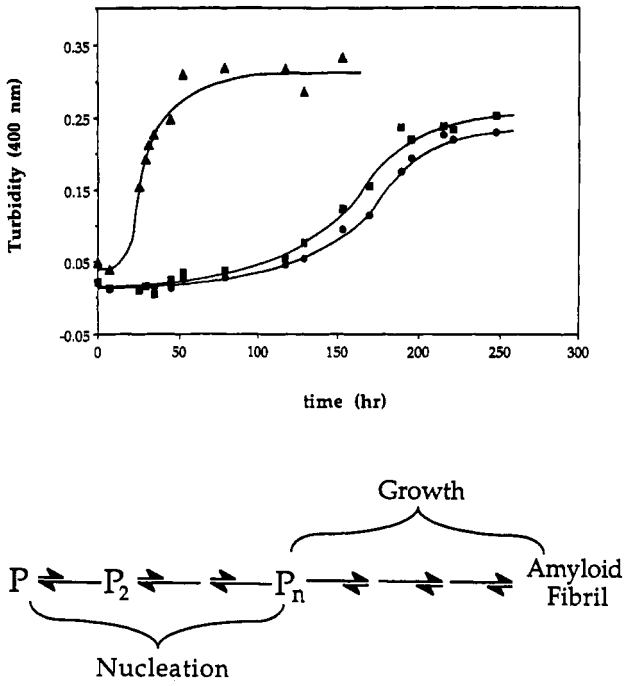

FIGURE 6: Aggregation of peptides at 425 μM in standard buffer as indicated by the turbidity of the solutions: (●) OsmB; (▲) OsmA; (■) OsmG3. The hypothetical mechanism demonstrates how slow formation of a nucleus leads to rapid and thermodynamically favored growth into an amyloid fibril.

inspection or measured turbidity. After this delay, the peptide would begin to aggregate, forming visible particles which were detected by a rise in the measured turbidity. The CD spectrum was measured for OsmB(28–44) at various points during the aggregation process. During the delay period, there was no change in the spectrum, which indicated a random-coil conformation. During the growth period, there was a decrease in the CD signal which generally correlated with the extent of aggregation, although no change in the shape of the CD spectrum was observed. The solubility of each peptide was measured after aggregation had apparently ceased (Figure 6): OsmB(28–44), 42 μM; OsmG3, 60 μM; and OsmA, 15 μM. Differences in the rates of nucleation and growth of the three peptide fibrils (Figure 6) may derive from the fact the extent of supersaturation (starting concentration/thermodynamic solubility) is different for each peptide (OsmB(28–44) = 10.1, OsmG3 = 7.1, OsmA = 28.3) (Eaton & Hofrichter, 1990).

Redissolution of the Fibrils Is Slow. Fibrils were formed by stirring a buffered solution of each peptide. Fibrils from each peptide were suspended in water and in fresh buffer. After the solutions were allowed to equilibrate for 5 days, the concentration of soluble peptide was determined. For OsmB-(28–44), the concentration was 46 μM in H_2O and 41 μM in buffer, similar to the solubility values obtained when supersaturated solutions were allowed to aggregate, indicating that the aggregation was reversible. For OsmG3, the concentration after redissolution was 23 μM in H_2O and 16 μM in buffer, while the solubility in H_2O was 83 μM and in buffer was 60 μM, demonstrating that the redissolution of this peptide was much slower than OsmB(28–44). For OsmA, the results were similar, with the concentration after 5 days of redissolution 4 μM in both water and buffer, while the solubility was 13 μM in H_2O and 15 μM in buffer. The redissolution of this peptide is slow, having reached only 25% of the equilibrium solubility after 5 days.

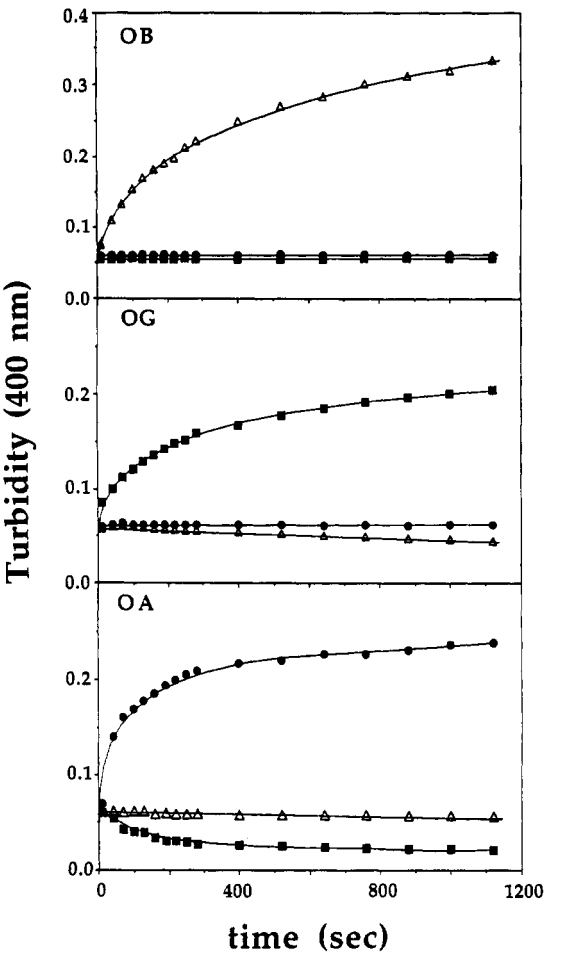

FIGURE 7: Nucleation of fibril growth. A total of 12.5 nmol of aggregated peptide was added to 1 mL of a 250 μM peptide solution. OB, OG, and OA indicate OsmB(28–44), OsmG3, and OsmA originally as a supersaturated solution. Symbols: (△) OsmB(28–44) fibrils added; (■) OsmG3 fibrils added; (●) OsmA fibrils added.

The Nucleation of Fibril Growth Is Rapid and Sequence Specific. Aggregated fibrils of each peptide were sonicated for 15 min to fragment the fibrils and expose fresh growth surfaces. Suspensions of these fibrils (50 μL, 12.5 nmol) were used to nucleate fibril growth from supersaturated solutions (950 μL, 250 μM) of each peptide (Figure 7). If an OsmB-(28–44) solution was seeded with OsmB(28–44) fibrils, growth occurred rapidly with $t_{1/2} \sim 300$ s. However, if an OsmB-(28–44) solution was seeded with OsmG3 or OsmA fibrils, the absorbance did not change over 30 min, indicating no fibril growth. Similar results were observed for both OsmG3 and OsmA solutions (Figure 7). None of the peptides show any aggregation over this short time span without seeding. The concentration of soluble peptide remaining after 30 min was ~150 μM for each peptide seeded with its own fibrils, although fibril growth had apparently stopped. Fibrils from OsmB(28–44) were sonicated for a longer period (~90 min) and added to a supersaturated solution of OsmB(28–44). The rate of fibril growth was similar, but the concentration of soluble peptide remaining after growth had stopped was ~90 μM, indicating that the extent of fibril growth is limited by the degree of fragmentation of the seed fibril suspension.

DISCUSSION

The molecular mechanisms which lead to the formation of insoluble amyloid fibrils and plaques are poorly understood. We have investigated the structure of amyloid comprising a

peptide derived from residues 34–42 of the β protein (Spencer et al., 1991; Halverson et al., 1990). The structure of this amyloid is unusual, and it suggests that amyloid structure may be more complex and varied than previously thought (Lansbury, 1992). Given the critical role which the glycine residues play in the structure of the β(34–42) peptide, we wondered whether similar sequences might play a role in the formation of amyloid plaques by other proteins. The periodic occurrence of glycine would impart greater conformational freedom on a peptide, allowing unusual conformations which could pack more efficiently in the fibril. In addition, we reasoned that the core of a fibril must contain few charged residues and will contain primarily hydrophobic residues, similar to the core of a globular protein (Richardson & Richardson, 1989). Finally, β-branched residues such as Val and Ile are sterically constrained to extended conformations and hence would be likely to populate β-sheet structures, which characterize many amyloids (Richardson & Richardson, 1989). A consensus sequence was developed on the basis of these criteria and used to search the sequence database for similar sequences. In addition to the β protein, 26 proteins were found to contain sequences of this type. One of these, the scrapie prion protein, is known to form amyloid fibrils (Stahl & Prusiner, 1991). A peptide derived from this sequence in the prion protein (PrP96–111, Figure 1) forms amyloid fibrils which are similar to those described herein (J. Come and P. T. Lansbury, Jr., unpublished results). The properties of the bacterial OsmB protein were unknown; therefore, a sequence from this protein (OsmB(28–44), Figure 1) was selected for further study (Jung et al., 1989). The peptide based on this sequence (OsmB(28–44)) and two control peptides, one to probe the importance of glycine (OsmA) and one to probe the importance of sequence (OsmG3) in amyloid fibril formation, are the subject of this study (Figure 2). The results detailed above show that neither of these factors is critical for amyloid formation but that the fibrils formed from these three sequences are demonstrably different.

The peptide OsmB(28–44) exists in aqueous solution as a mixture of rapidly interconverting conformers over a large concentration range (10–1000 μM), with CD spectra similar to that observed at 100 μM (Figure 3). Supersaturated solutions show no evidence of a soluble, structured peptide. As the peptide concentration was increased to 1 mM in water, each of the peptides spontaneously formed an insoluble gel/fibrillar suspension. At lower concentrations, supersaturated peptide solutions appeared to be stable and free from aggregate for hours to days. However, we found that stirring or sonication of these solutions resulted in rapid formation of an aggregate. Aggregation due to agitation was recently observed in the case of insulin (Sluzky et al., 1991). The authors demonstrated that the elimination of hydrophobic surfaces such as the air/water interface and/or Teflon prevents the aggregation of insulin. However, agitation of OsmB(28–44) after the elimination of air and the Teflon stir bar resulted in aggregation similar to that observed previously. After supersaturated solutions were stirred for several hours, no further aggregation was detectable. The solubility of each peptide measured under these conditions may represent the thermodynamic solubility of these peptides. OsmA was determined to be the least soluble of the three peptides, consistent with its greater hydrophobicity. The rate of dissolution of the peptide amyloids was very slow; in the case of OsmG3 and OsmA the thermodynamic solubility was not reached after 5 days. This suggests that the rate of monomer dissociation from the peptide aggregate may be very slow, which is a partial explanation for the low solubility. As a result, one must be very careful when making solubility measurements to be certain that kinetic barriers are overcome and thermodynamic solubility is attained.

Peptide amyloid fibrils contained β-sheet structure as shown by the vibrational absorption band at $\sim$1630 cm^{-1} (Figure 4) (Krimm & Bandekar, 1986). The absorption band at $\sim$1665 cm^{-1} may indicate the presence of a β-turn, but other authors have shown that the assignment of bands in this region is not straightforward (Wilder et al., 1992). While the general positions of the bands are similar for all three peptides, there are slight differences in the band shape, which may indicate significant differences at the molecular level (Lansbury, 1992). The fibrillar peptide aggregates all bind Congo red, despite the absence of charged residues, suggesting that this binding is primarily due to hydrophobic interactions (Cooper, 1974; Klunk et al., 1989). OsmB(28–44) and OsmA show birefringence while OsmG3 does not. Again, this suggests the existence of subtle differences in the structure of these fibrillar aggregates despite the similarity in other physical properties between OsmB(28–44) and OsmG3. The fibrils obtained from each peptide were similar in dimension (Figure 5); however, the morphology of these fibrils varied considerably, indicating that the subtle differences in structure discussed above affect the fibrillar morphology.

In order to determine if the peptide sequence affects the rate of fibril formation in addition to the structure of the peptide fibril, the turbidity of supersaturated solutions of each peptide was monitored for several weeks (Figure 6). Turbidity has been used to monitor sickle-cell hemoglobin aggregation (Eaton & Hofrichter, 1990) and has been shown to be proportional to the mass of the aggregate in dilute suspensions (Berne, 1974). All solutions exhibited a delay period during which no aggregation was observed. The CD spectrum of the solution did not change during this period, indicating structured soluble aggregates were not present in significant amounts. The delay period (5–8 h for OsmA and 4–5 days for OsmB-(28–44) and OsmG3) was followed by a period of growth, during which time both the measured turbidity and the observed viscosity of the solutions increased dramatically. After growth, the turbidity remained constant for several days and then decreased as the aggregates coalesced into a few larger particles which scatter less light (Beaven et al., 1969). During the growth period, the shape of the CD spectrum remained the same as that in aqueous buffer, yet the intensity was reduced. This suggests that the aggregate does not contribute to the CD signal and that the concentration of soluble aggregates is very low. This kinetic behavior, characterized by a lag period during which nuclei are slowly forming, followed by a period of rapid growth, is typical of crystal formation (Kam et al., 1978). Similar kinetics have been observed for the aggregation of glucagon (Beaven et al., 1969) and the aggregation of sickle-cell hemoglobin (Eaton & Hofrichter, 1990). In the case of sickle-cell hemoglobin, the monomers are believed to aggregate very slowly until a nucleus of ca. 20–30 monomers is attained, at which point fibril growth is spontaneous and very fast. The rate of formation of a 20-mer nucleus is proportional to the monomer concentration to the 19th power (Eaton & Hofrichter, 1990; Hofrichter et al., 1974). Consequently, aggregation of sickle-cell hemoglobin is very sensitive to the monomer concentration; a slight increase in concentration results in a dramatic decrease in the nucleation time (Hofrichter et al., 1974). The consequences of crystallization kinetics on in vivo amyloidogenesis will be discussed below.

The long delay period observed for the aggregation of each peptide suggests that the rate-limiting step in fibril formation is the formation of a stable nucleus which acts as a template for rapid fibril growth. The addition of nuclei to a supersaturated solution results in spontaneous fibril growth, analogous to the seeding of crystallization. This effect has been shown to occur in vitro with murine senile amyloid fibrils (Naiki et al., 1991). Furthermore, the injection of sonicated AA-amyloid fibrils into hamsters resulted in experimentally induced amyloidosis after 4 days, a significant decrease from the normal incubation time of 2 weeks; this may reflect an in vivo nucleation phenomenon (Niewold et al., 1987). We generated nuclei by sonicating peptide fibrils and added these to a supersaturated solution of each peptide. The turbidity of the seeded solutions increased rapidly (Figure 7). The unnucleated aggregation of OsmB(28–44) requires >100 h to reach a stable endpoint. However, when the same solution is nucleated by addition of sonicated fibrils, growth is much faster, reaching an endpoint after 30 min. This evidence suggests that the rate-limiting step in spontaneous fibril growth is the formation of a nucleus (Figure 6). Further growth of the fibril is fast and spontaneous.

This nucleation effect was found to be sensitive to peptide sequence. While immediate growth was observed if OsmB(28–44) fibrils were added to a supersaturated OsmB(28–44) solution, addition of OsmG3 or OsmA fibrils resulted in no growth (Figure 7). The same result was observed for supersaturated OsmG3 and OsmA solutions; the aggregation of each peptide could only be nucleated by addition of its own fibrils. This sequence specificity confirms that the fibrils from each peptide have slightly different structure and that fibril nucleation requires specific intermolecular hydrophobic interactions.

CONCLUSIONS

We have shown that a peptide derived from the OsmB protein sequence spontaneously forms amyloid fibrils in vitro. Since 70% of the protein is composed of a sequence similar to this peptide, it is likely that the OsmB protein would also be capable of forming amyloid-like fibrils. Fibril formation from a supersaturated solution of the peptide OsmB(28–44) involves a significant lag time, reflecting the kinetic barrier to amyloid formation. The length of the lag time may be extremely sensitive to peptide concentration. The OsmB protein is bound to the outer membrane through a lipid attachment, and under the conditions of osmotic shock which induce increased expression, the protein may be concentrated sufficiently at the membrane surface to initiate amyloid formation. OsmB amyloid may reinforce the bacterial outer membrane, protecting the cell and inhibiting cell division (Jung et al., 1989).

The crystallization kinetics demonstrated herein may also have important consequences on amyloidogenesis in Alzheimer's disease. Rate-determining nucleation is highly dependent on monomer concentration. Assuming that 21 molecules are required to form a nucleus, a 5% increase in the monomer concentration could result in a 2.6-fold increase in the rate of aggregation (1.05^{20}) (Eaton & Hofrichter, 1990; Hofrichter et al., 1974). Similarly, 10% and 50% increases in monomer concentration could result in aggregation rate increases of ca. 7-fold and ca. 3000-fold, respectively! This example demonstrates how small concentration increases, whether of OsmB at the membrane surface in response to osmotic shock or of the β amyloid protein in the lysosome as a result of altered processing (Haass et al., 1992), can greatly increase the rate of amyloid formation. With respect to AD, the possibility exists that an endogenous inhibitor, defective in the diseased brain, may normally prevent nucleation. On the other hand, the AD brain may contain a material which could act as a heterogeneous nucleator and greatly increase the rate of amyloid formation.

The sequence of OsmB(28–44) is similar to the C-terminal region of the β protein from Alzheimer's disease and a sequence from the scrapie prion protein (PrP96–111). We have shown that this peptide and related peptides form amyloid fibrils. While the properties of the control peptides suggest that a specific sequence may not be critical in amyloid formation, sequence similarities (e.g., β-branched residues interspersed with flexible Gly residues) may be important. Slight differences in fibril morphology (EM), peptide structure (FTIR), and Congo red staining and birefringence reflect subtle differences at the molecular level; however, these differences are not interpretable (Lansbury, 1992). The sequence specificity of the nucleation event also suggests that the amyloid fibrils differ at the molecular level and that nucleation involves a precise intermolecular recognition event. Finally, we have shown that aggregation occurs according to nucleation and growth kinetics and that nucleation is the rate-limiting step in the aggregation process.

REFERENCES

Ananthanarayanan, V. S., Andreatta, R. H., Poland, D., & Scheraga, H. A. (1971) *Macromolecules 4*, 417.

Beaven, G. H., Gratzer, W. B., & Davies, H. G. (1969) *European J. Biochem. 11*, 37.

Berne, B. J. (1974) *J. Mol. Biol. 89*, 755.

Burdick, D., Soreghan, B., Kwon, M., Kosmoski, J., Knauer, M., Henschen, A., Yates, J., Cotman, C., & Glabe, C. (1992) *J. Biol. Chem. 267*, 546.

Chou, K.-C., Pottle, M., Nemethy, G., Ueda, Y., & Scheraga, H. A. (1982) *J. Mol. Biol. 162*, 89.

Chou, P. Y., & Fasman, G. D. (1978) *Adv. Enzymol. Relat. Areas Mol. Biol. 47*, 45.

Cooper, J. H. (1974) *Lab. Invest. 31*, 232.

Dyrks, T., Weidemann, A., Multhaup, G., Salbaum, J. M., Lemaire, H.-G., Kang, J., Muller-Hill, B., Masters, C. L., & Beyreuther, K. (1988) *EMBO J. 7*, 949.

Eaton, W. A., & Hofrichter, J. (1990) *Adv. Protein Chem. 40*, 63.

Fraser, R. D. B., & MacRae, T. P. (1973) in *Conformation in Fibrous Proteins and Related Synthetic Polypeptides*, Ch. 13, Academic Press, New York.

Glenner, G. G., & Wong, C. W. (1984) *Biochem. Biophys. Res. Commun. 120*, 885.

Greenfield, N., & Fasman, G. D. (1969) *Biochemistry 8*, 4108.

Haass, C., Koo, E. H., Mellon, A., Hung, A. Y., & Selkoe, D. J. (1992) *Nature 357*, 500.

Halverson, K., Fraser, P. E., Kirschner, D. A., & P. T. Lansbury, J. (1990) *Biochemistry 29*, 2639.

Hilbich, C., Kisters-Woike, B., Reed, J., Masters, C. L., & Beyreuther, K. (1991) *J. Mol. Biol. 218*, 149.

Hofrichter, J., Ross, P. D., & Eaton, W. A. (1974) *Proc. Natl. Acad. Sci. U.S.A. 71*, 4864.

Jung, J. U., Gutierrez, C., & Villarejo, M. R. (1989) *J. Bacteriol. 171*, 511.

Kaiser, E., Colescott, R. L., Bossinger, C. D., & Cook, P. I. (1970) *Anal. Biochem. 54*, 595.

Kam, Z., Shore, H. B., & Feher, G. (1978) *J. Mol. Biol. 123*, 539.

Kang, J., Lemaire, H.-G., Unterbeck, A., Salbaum, J. M., Masters, C. L., Grzeschik, K.-H., Multhaup, G., Beyreuther, K., & Müller-Hill, B. (1987) *Nature 324*, 733.

Klunk, W. E., Pettegrew, J. W., & Abraham, D. J. (1989) *J. Histochem. Cytochem. 37*, 1273.

Krimm, S., & Bandekar, J. (1986) *Adv. Protein Chem. 38*, 181.
Kyte, J., & Doolittle, R. F. (1982) *J. Mol. Biol. 157*, 105.
Lansbury, P. T., Jr. (1992) *Biochemistry 31*, 6865.
Marqusee, S., Robbins, V. H., & Baldwin, R. L. (1989) *Proc. Natl. Acad. Sci. U.S.A. 86*, 5286.
Masters, C. L., Simms, G., Weinman, N. A., Multhaup, G., McDonald, B. L., & Beyreuther, K. (1985) *Proc. Natl. Acad. Sci. U.S.A. 82*, 4245.
Morrisett, J. D., David, J. S. K., Pownall, H. J., & Antonio M. Gotto, J. (1973) *Biochemistry 12*, 1290.
Naiki, H., Higuchi, K., Nakakuki, K., & Takeda, T. (1991) *Lab. Invest. 65*, 104.
Niewold, T. A., Hol, P. R., Andel, A. C. J. v., Lutz, E. T. G., & Gruys, E. (1987) *Lab. Invest. 56*, 544.
Sluzky, V., Tamada, J. A., Klibanov, A. M., & Langer, R. (1991) *Proc. Natl. Acad. Sci. U.S.A. 88*, 9377.
Smith, P. K., Krohn, R. I., Hermanson, G. T., Mallia, A. K., Gartner, F. H., Provenzano, M. D., Fujimoto, E. K., Goeke, N. M., Olson, B. J., & Klenk, D. C. (1985) *Anal. Biochem. 150*, 76.
Spencer, R. G. S., Halverson, K. J., Augér, M., McDermott, A. E., Griffin, R. G., & Lansbury, P. T., Jr. (1991) *Biochemistry 30*, 10382.
Stahl, N., & Prusiner, S. B. (1991) *FASEB J. 5*, 2799.
Wilder, C. L., Friedrich, A. D., Potts, R. O., Daumy, G. O., & Francoeur, M. L. (1992) *Biochemistry 31*, 27.

Registry No. OsmB(28–44), 144375-61-1.